CHINESE OPTICS LETTERS
Vol. 20, No. 4 | April 2022

# Femtosecond-laser-induced backward transfer of fluorinated ethylene propylene for fabrication of "lotus effect" surfaces

Kongyu Lou (娄孔昱)[1,2], Jing Qian (钱 静)[1,2], Xiaohan Yu (于潇涵)[1,3], Zhaoyuan Xia (夏照远)[1,2], Danyang Shen (沈丹阳)[1,2], Guande Wang (王关德)[1,2], and Quan-Zhong Zhao (赵全忠)[1,2*]

[1] State Key Laboratory of High Field Laser Physics and CAS Center for Excellence in Ultra-intense Laser Science, Shanghai Institute of Optics and Fine Mechanics, Chinese Academy of Sciences, Shanghai 201800, China

[2] Center of Materials Science and Optoelectronics Engineering, University of Chinese Academy of Sciences, Beijing 100049, China

[3] MOE Key Laboratory of Advanced Micro-Structured Materials, School of Physics Science and Engineering, Tongji University, Shanghai 200092, China

*Corresponding author: zqz@siom.ac.cn

Received November 15, 2021 | Accepted January 18, 2022 | Posted Online February 18, 2022

**"Lotus effect" glass surfaces with fluorinated ethylene propylene were successfully fabricated by using a femtosecond laser-induced backward transfer (LIBT) method. By space-selectively modifying both the surface morphology and surface chemistry in a single step, LIBT provides a convenient and flexible route to fabricate superhydrophobic surfaces with ultra-low adhesion. A systematic mechanism responsible for the anisotropic wetting behaviors and adhesion modulation was proposed with a combination of the Cassie and Wenzel models. X-ray photoelectron spectroscopy revealed that oxidation and defluorination were induced by laser radiation. LIBT is proved to be a promising method for programmable manipulations of functional surfaces with diverse wettability.**

**Keywords:** superhydrophobic surface; laser-induced backward transfer; fluorinated ethylene propylene; glass.
**DOI:** 10.3788/COL202220.043801

## 1. Introduction

Superhydrophobicity, which indicates a water contact angle (CA) of more than 150°, is a common property in nature[1]. The Lotus effect, as a special type of superhydrophobicity, attracted enormous attention due to its low adhesion, which has been successfully used for self-cleaning, anti-corrosion, antisepsis, non-fouling, chemical shielding, oil-water separation, etc.[2–9].

Superhydrophobicity is believed to be a physiochemical phenomenon that depends on two key aspects: surface energy and surface microstructures[10,11]. For fabricating "lotus effect" surfaces, versatile methods have been applied. For example, laser direct writing was used to produce micro-protrusion array structures on surfaces of alloy[12]; spray coating technology was used to assemble silicone-based paint into films on solid substrates[13]; the lithography method was used to print a petal-like structure on preprocessed wood, which was firstly placed into the precursor PVB/$SiO_2$ solutions[14]. But, laser direct writing and spray coating can only modify surface microstructures and surface chemistry, respectively. For the lithography method, multi-steps including stamp preparation, solvothermal processing, and nanoimprint processing were even applied, which was somewhat complex and cost expensive. Despite the already used techniques, there is still a great demand for a more convenient and flexible route to fabricate "lotus effect" surfaces. In addition, further reduction of surface adhesion to the extent that the sliding angle of a water droplet approaches zero is still a great challenge ahead.

Laser-induced backward transfer (LIBT) is an emerging technology that enables space selective modification of both the surface microstructures and surface chemistry in a single step. LIBT was first reported, to the best of our knowledge, by Bohandy *et al.*[15], in which Cu was transferred from metal plates to a silicon plate. Nowadays, LIBT is commonly used for microprinting of diffractive optical structures and computer-generated holograms, writing active and passive mesoscopic circuit elements, producing nanoparticles and 3D microstructures, as well as for biomolecule printing applications, etc.[16,17]. However, LIBT has rarely been used for the fabrication of "lotus effect" surfaces. In order to obtain superhydrophobic surfaces by the LIBT process, receiving substrates are only required to be transmissive for lasers. Ordinary commercial glass can easily meet the demand. In contrast, donor substrates should be prudently considered so as to achieve the desired wettability. Fluorinated ethylene propylene (FEP) is a typical fluoride with low surface energy and has been previously used for fabricating superhydrophobic surfaces by utilizing hot embossing, UV radiation, etc.[18,19]. However, these methods can only fabricate superhydrophobicity on materials with low surface energy. To the best of our knowledge, FEP has scarcely been designed for superhydrophobicity by femtosecond (fs) laser direct writing or by the LIBT method. Therefore, FEP was selected as the donor substrate.

In this study, LIBT was successfully used to fabricate "lotus effect" surfaces by enhancing roughness and coating a thin layer of FEP on glass surfaces. With CAs improved to more than 150°, surface adhesion was further reduced down to the minimum that a 5 μL water droplet could not stick onto the glass surface. The dependence of anisotropic wetting behaviors and adhesion modulation on laser power and scanning interval was systematically investigated, and a combination of the Wenzel and Cassie models was proposed to evaluate the wetting performances. Combined with high-power lasers and high-speed scanning systems, LIBT is expected to be an advanced manufacturing method for large-scale fabrication of superhydrophobic surfaces with high-processing resolution.

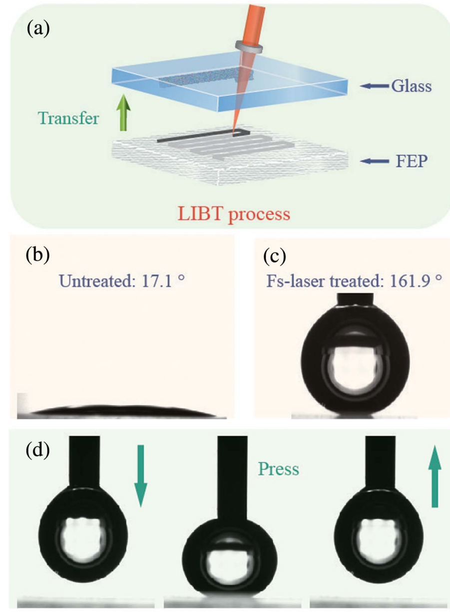


**Fig. 1.** (a) Schematic diagram of LIBT process; the side view of a 5 μL pure water droplet on the glass surface (b) before and (c) after the LIBT process; (d) the surface repelled a 5 μL droplet (laser power: 0.8 W; scanning interval: 10 μm). The green arrows represent the moving direction of the needle.

## 2. Experiment

FEP films with a thickness of 200 μm were used as the donor substrates. The receiving substrates were soda lime microscope slides with dimensions of 76 mm × 25 mm × 1 mm. A fs laser (Pharos-SP-10W, Light Conversion) with wavelength of 1030 nm, pulse width of 182 fs, and pulse frequency of 100 kHz was used for LIBT. As shown in Fig. 1(a), the FEP film was tightly bonded to the glass surfaces, and, after transmitting through the glass (receiver), the fs laser was focused onto the interface between the glass and FEP films (donor) by a 10× objective lens (NA = 0.3). FEP films were then transferred to the glass substrate by implementing a parallel line raster pattern process. The laser scanning speed was set at 20 mm/s, and the scanning interval was varied from 10 to 70 μm. Using LIBT, the morphology and chemical components of the glass surface were modified at the same time.

The morphology of the glass surface was revealed via an optical microscope (VHX-7100, Keyence) and a scanning electron microscope (SU8100, Hitachi). The CAs were measured by specific equipment (SL200B, Kino), and a 5 μL water droplet was captured by a commercial CCD (EM-MV-200C, Microvision). In addition, chemical components of the glass surface were analyzed by X-ray photoelectron spectroscopy (XPS, Thermo Scientific Escalab 250xi).

## 3. Results and Discussion

The CAs before and after the LIBT process are compared in Figs. 1(b) and 1(c). Before the LIBT process, the glass surface was hydrophilic with a CA of 17.1°. However, when proper laser parameters were selected, the glass surface was roughened and, at the same time, coated by a thin FEP layer. As a result, the CA increased to 161.9°. More importantly, a 5 μL water droplet could easily leave the surface with the rising needle even pressing it [Fig. 1(d)], indicating extreme water repellence. Therefore, the LIBT process has transformed a hydrophilic adhesive glass surface into a superhydrophobic non-adhesive glass surface, which is a typical "lotus effect." The hydrophobicity remained stable after 3 months.

The dependence of water CAs on laser power at the scanning intervals of 10 μm, 30 μm, 50 μm, and 70 μm is shown in Figs. 2(a)–2(d). To test the anisotropic wettability, the static water CAs in two vertical directions, which were defined as the parallel direction and perpendicular direction with respect to the scanning line, were measured. At a scanning interval of 10 μm, the CAs of more than 150° could be achieved within laser power of 0.5–1.5 W, and there was little difference of CAs in the two vertical directions [Fig. 2(a)]. As mentioned in Fig. 1(c), when CAs reach more than 150°, the surface adhesion becomes so low that sticking of droplets on superhydrophobic glass could not be achieved. Therefore, in addition to CAs measured in two vertical directions in Fig. 2, a third label of a green cross is introduced to indicate ultralow adhesion. When the scanning interval was increased to 30 μm, CAs of more than 150° could only be achieved within a much smaller range of laser power (0.7–0.9 W). Besides, an apparent difference of CAs measured in the two vertical directions existed. With the scanning interval further increasing to 50 μm and 70 μm, the proper range of laser power to achieve superhydrophobicity was further reduced, and the difference value of CAs between two vertical directions was

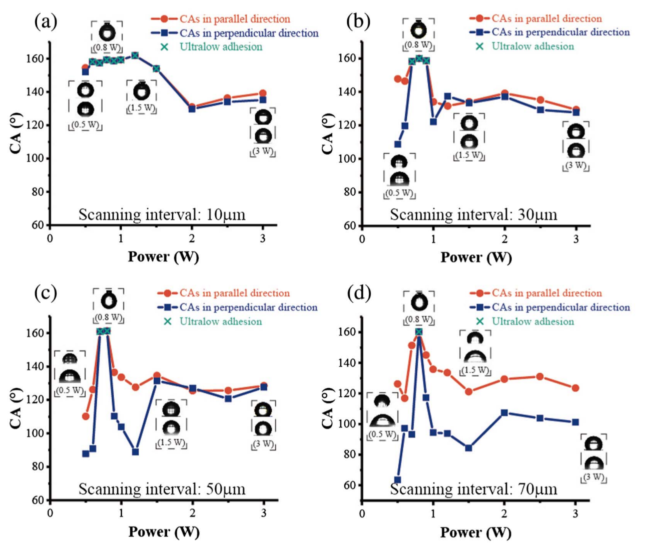


**Fig. 2.** Dependence of CAs on laser power at scanning intervals of (a) 10 μm, (b) 30 μm, (c) 50 μm, and (d) 70 μm (water droplet: 5 μL).

further enhanced. It can be seen that when the scanning interval was 70 μm, CAs of more than 150° could only be obtained at the optimum laser power of 0.8 W. Except for the optimal laser power, there was a large degree of difference of CAs measured along the two vertical directions within laser power of 0.5–3 W. The results above demonstrate that for each scanning interval, a laser-power window for superhydrophobicity exists. As long as the appropriate laser parameters are selected, glass surfaces with the “lotus effect” can be simply obtained by the LIBT process.

The effect of surface morphology on wettability is illustrated in Fig. 3. When the scanning interval was 10 μm, all scanning lines overlapped with each other so that the whole glass surface was covered by a thin layer of FEP. However, when the scanning interval was further increased to 30 μm, 50 μm, and 70 μm, no overlapping of scanning lines could be seen, and anisotropic wettability became apparent. At a laser power of 0.5 W, the FEP layer transferred to the glass surface stayed relatively neat. When the laser power was 0.8 W, fluctuations in the density and altitude generated by impact stress began to appear around the scanning lines [Figs. 3(i)–3(l)][20–22] and then became stronger with increasing laser power [Figs. 3(a)–3(h)]. From the whole evolution of wetting ability, we can find that the scanning interval is the most important factor accounting for anisotropic wettability, which will be systematically discussed in the following section.

Component analysis of the surfaces was performed using XPS. The initial glass and pristine FEP were also XPS-analyzed for comparison [Fig. 4(a)]. The peaks of F 1s and C 1s on the treated glass surfaces confirmed the presence of carbon and fluorine, which was evidence that FEP was successfully transferred. Another two obvious peaks of Na 1s and O 1s were the intrinsic signals of soda lime microscope slides. Considering the nanoscale penetration depth of XPS, we can assume that the thickness of the FEP layer was approximately 10 nm. To further confirm that the chemical groups transferred onto the glass surface, curve fittings of C 1s peak for FEP, and for glass surfaces treated at varied laser powers are compared in Figs. 4(b)–4(d). In addition, each deconvolution band of C 1s peak was assigned to its corresponding chemical groups, and their relevant percentage was calculated in Table 1[19,23–26]. In pristine FEP, $(-C^{*}F_2-CF_2-)_n$ at 292 eV was the dominant chemical group. Due to the photo-oxidation effect, a new chemical group of $CF-O-C^{*}F_2$ began to appear at the laser power of 0.5 W. With the laser power further increased to 3 W, $CF-O-C^{*}F_2$ became the prevalent chemical

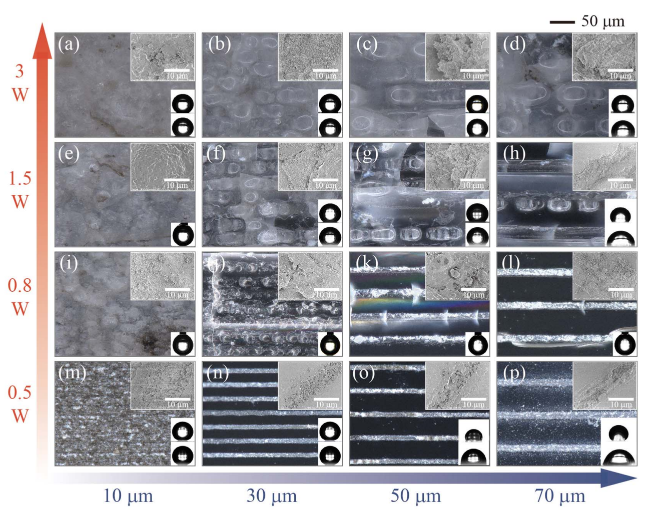


**Fig. 3.** Evolution of morphology and wetting ability of glass surface treated by the LIBT process with varied laser power and scanning intervals. Insets: SEM images with higher magnifications and snapshots of 5 μL water droplet on the glass surface along parallel (upper) and perpendicular (bottom) directions.

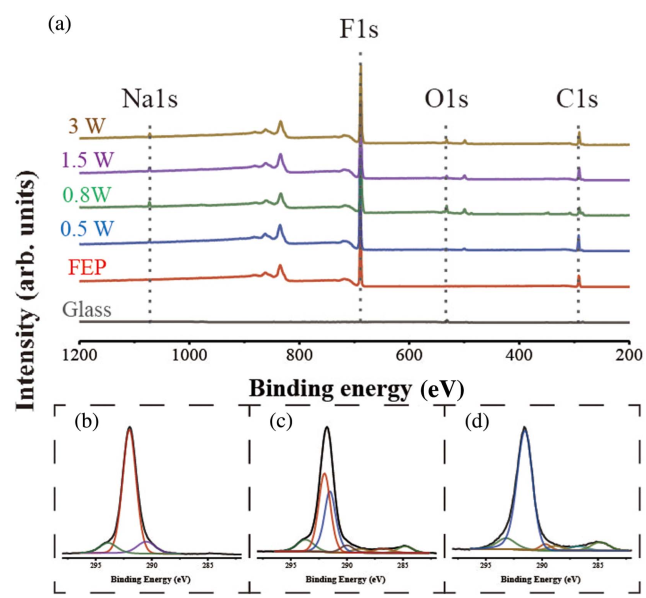


**Fig. 4.** (a) XPS analysis of the initial glass, pristine FEP, and the glass surfaces after the LIBT process at varied laser powers; curve fittings of C 1s peak for (b) pristine FEP and treated glass surfaces at the laser power of (c) 0.5 W and (d) 3 W.

**Table 1.** Curve Fittings of C 1s Peak (in atomic fraction, %) for FEP and Glass Surface Treated by LIBT Process.

| | Binding Energy (eV) | Assignment | Fraction (%) |
|---|---|---|---|
| FEP | 292 | $(-C^*F_2-CF_2-)_n$ | 81.6 |
| | 290.5 | $(-C^*F_2-CH_2-)_n$ | 10.63 |
| | 293.9 | $C^*F_3$ | 8.21 |
| | 292 | $(-C^*F_2-CF_2-)_n$ | 42.46 |
| 0.5 W | 291.5 | $CF-O-C^*F_2$ | 33.55 |
| | 293.7 | $C^*F_3$ | 9.01 |
| | 284.8 | C–C | 4.43 |
| | 290 | $C^*F$ | 4.3 |
| | 286.77 | $(-CF_2-C^*H_2-)_n$ | 3.41 |
| | 288.8 | C = O | 2.85 |
| 3 W | 291.5 | $CF-O-C^*F_2$ | 76.53 |
| | 293.2 | $C^*F_3$ | 8.59 |
| | 284.8 | C–C | 6.08 |
| | 286.77 | $(-CF_2-C^*H_2-)_n$ | 3.09 |
| | 289.7 | $-C^*F-CF_2-CF_3$ | 2.8 |
| | 288.8 | C = O | 2.91 |

group at a percentage of 76.53%. Moreover, several weak peaks within the range of 284.8 eV to 290 eV also appeared, which indicated that the photo-oxidation effect was also accompanied by a small degree of defluorination during the LIBT process[23,27].

Therefore, LIBT is like a coating method, however it possesses fascinating advantages for fabricating the bionic lotus effect, (i) modifying both surface roughness and surface energy in a single step. Once absorption of light occurred at the interface, heating-induced melting of both FEP and glass was localized. Due to the difference of the melting threshold, the glass surface was minimally roughened, and a thin layer of FEP film was transferred onto the glass surface by vapor-driven propulsion, thus reducing surface energy, with (ii) large-scale fabrication of micro-scale resolution. In the LIBT process, a focusing lens was used to precisely control where structural modification occurs, and the line width of the FEP film transferred onto the glass surface could be reduced down to the micron dimension. The combination of high-power lasers and high-speed scanning systems could enable large-scale fabrication of the superhydrophobic surface quickly and accurately by LIBT being (iii) with low cost and ecofriendly. In the LIBT process, the receiving and donor substrates are commonly used commercial soda lime microscope slides and polymer material (FEP). Moreover, the pulse's energy deposited over the time scale of

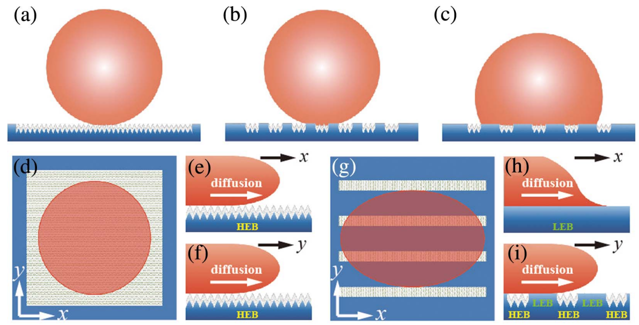


**Fig. 5.** (a)–(c) Schematic illustrations of wetting states at different intervals. Top view of a water droplet on glass surface after LIBT process at (d) small and (g) large intervals; side view of water diffusion on glass surface in the direction (e), (h) parallel and (f), (i) perpendicular to scanning lines (HEB, high-energy barriers; LEB, low-energy barriers).

fs ensured a minimal amount of heating and melting, with no harmful substances spraying into the air.

During the LIBT process, laser radiation, on the one hand, provides the driving force for FEP transfer and, on the other hand, causes oxidation and defluorination. FEP transferred onto the glass surface enhances wettability owing to its low surface energy[23]. However, both oxidation and defluorination cause higher surface energy, which degrades water repellency[23]. The two factors compete with each other, so an optimum laser-power window exists for superhydrophobicity, which has been clearly illustrated in Fig. 2.

The influence of scanning interval is discussed as follows. As mentioned in Fig. 1(b), an initial glass surface exhibits hydrophilicity and high adhesion, which is a typical Wenzel state. When the entire glass surface is coated with a thin layer of FEP using LIBT [as shown in Fig. 3(i)], the hierarchic structure of FEP film traps air under the water, leading to the Cassie–Baxter wetting behavior. On the basis of the above mentioned, we propose a mechanism responsible for the wetting states at different intervals in Fig. 5.

When the scanning interval was so small that the transferred FEP films overlapped with each other, it led to a typical Cassie–Baxter wetting behavior [Fig. 5(a)]. In this state, superhydrophobicity with ultralow adhesion can be readily obtained at a large range of laser powers. However, with an increase of interval, the uncovered zone by FEP film increases, and Wenzel states gradually dominate the wetting performance, which results in lower CAs and larger adhesion [Fig. 5(c)]. Anisotropic wettability can also be explained by this model, as depicted in Figs. 5(d)–5(i). Energy barriers (EBs) are an influential factor for water diffusion[28,29]. In this experiment, EBs of the FEP coated zone were larger than that of the uncovered area. In the case of Fig. 5(a), the EBs are almost the same in two vertical directions [Figs. 5(d)–5(f)]. Therefore, a water droplet on the glass surface exhibited a nearly perfect sphere with negligible anisotropy. In the case of Fig. 5(c), water only needs to overcome low-EBs in the direction parallel to scanning lines [Fig. 5(h)]. In contrast, both low and high-EBs have to be conquered in the direction perpendicular to scanning lines [Fig. 5(i)]. As a result, CAs measured in Fig. 5(i) are higher than that in Fig. 5(h)[30].

## 4. Conclusion

In this paper, LIBT was successfully used to fabricate the "lotus effect" surface on superhydrophilic glass. The glass surface was roughened and coated by a thin layer of FEP in a single step, resulting in strong water repellence and extremely weak adhesion. It was proved that the larger the scanning interval was, much more apparent anisotropic wetting behaviors and much weaker hydrophobicity could be seen. Laser radiation provides a driving force for FEP transfer. However, XPS revealed that laser radiation also induces oxidation and defluorination, which are both adverse factors for wetting ability. Therefore, hydrophobic performance of the glass surface exhibited a nonlinear relationship with laser power. Anyway, for each scanning interval, there still exists an optimum laser-power window for superhydrophobicity. In addition, a combination of the Cassie and Wenzel models was proposed for explaining anisotropic wetting behaviors and adhesion modification. Due to its ability of large-scale fabrication with high-processing resolution, LIBT would be a promising method for fabricating functional surfaces with diverse wettability.

## Acknowledgement

This work was supported by the Shanghai Sailing Program (No. 20YF1455200) and the National Natural Science Foundation of China (NSFC) (No. 12104470).

## References

1. Y. Shao, J. Zhao, Y. Fan, Z. Wan, L. Lu, Z. Zhang, W. Ming, and L. Ren, "Shape memory superhydrophobic surface with switchable transition between 'lotus effect' to 'rose petal effect,'" Chem. Eng. J. **382**, 122989 (2020).
2. X. Yun, Z. Xiong, Y. He, and X. Wang, "Superhydrophobic lotus-leaf-like surface made from reduced graphene oxide through soft-lithographic duplication," RSC Adv. **10**, 5478 (2020).
3. S. P. Dalawai, M. A. S. Aly, S. S. Latthe, R. Xing, R. S. Sutar, S. Nagappan, C.-S. Ha, K. K. Sadasivuni, and S. Liu, "Recent advances in durability of superhydrophobic self-cleaning technology: a critical review," Prog. Org. Coat. **138**, 105381 (2020).
4. Y. Ye, D. Zhang, J. Li, T. Liu, J. Pu, H. Zhao, and L. Wang, "One-step synthesis of superhydrophobic polyhedral oligomeric silsesquioxane-graphene oxide and its application in anti-corrosion and anti-wear fields," Corros. Sci. **147**, 9 (2019).
5. K. D. Esmeryan, C. E. Castano, T. A. Chaushev, R. Mohammadi, and T. G. Vladkova, "Silver-doped superhydrophobic carbon soot coatings with enhanced wear resistance and anti-microbial performance," Colloid Surface A. **582**, 123880 (2019).
6. R. Jiang, L. Hao, L. Song, L. Tian, Y. Fan, J. Zhao, C. Liu, W. Ming, and L. Ren, "Lotus-leaf-inspired non-fouling, mechanical bactericidal surfaces," Chem. Eng. J. **398**, 125609 (2020).
7. L.-C. Jia, G. Zhang, L. Xu, W.-J. Sun, G.-J. Zhong, J. Lei, D.-X. Yan, and Z. Li, "Robustly superhydrophobic conductive textile for efficient electromagnetic interference shielding," Appl. Mater. Interfaces **11**, 1680 (2019).
8. X. Wang, Y. Pan, X. Liu, H. Liu, N. Li, C. Liu, D. W. Schubert, and C. Shen, "Facile fabrication of superhydrophobic and eco-friendly poly (lactic acid) foam for oil-water separation via skin peeling," Appl. Mater. Interfaces **11**, 14362 (2019).
9. C. Wang, B. Liu, Z. Luo, K. Ding, and J. Duan, "Fabrication of microholes array on titanium foil by a femtosecond laser and a surface's wettability switching," Chin. Opt. Lett. **19**, 082201 (2021).
10. R. N. Wenzel, "Resistance of solid surfaces to wetting by water," Ind. Eng. Chem. Res. **28**, 988 (1936).
11. A. Cassie and S. Baxter, "Wettability of porous surfaces," Trans. Faraday Soc. **40**, 546 (1944).
12. G. Xin, C. Wu, W. Liu, Y. Rong, and Y. Huang, "Anti-corrosion superhydrophobic surfaces of Al alloy based on micro-protrusion array structure fabricated by laser direct writing," J. Alloy. Compd. **881**, 160649 (2021).
13. C. Cao, B. Yi, J. Zhang, C. Hou, Z. Wang, G. Lu, X. Huang, and X. Yao, "Sprayable superhydrophobic coating with high processibility and rapid damage-healing nature," Chem. Eng. J. **392**, 124834 (2020).
14. Y. Yang, H. He, Y. Li, and J. Qiu, "Using nanoimprint lithography to create robust, buoyant, superhydrophobic PVB/$SiO_2$ coatings on wood surfaces inspired by red roses petal," Sci. Rep. **9**, 9961 (2019).
15. F. Adrian, J. Bohandy, B. Kim, and A. N. Jette, "A study of the mechanism of metal deposition by the laser-induced forward transfer process," J. Vac. Sci. Tech. B **5**, 1490 (1987).
16. P. Serra and A Piqué, "Laser-induced forward transfer: fundamentals and applications," Adv. Mater. Technol. **4**, 1800099 (2019).
17. X. Xu, J. Li, X. Yang, S. Pan, and Y. Bi, "Introduction of Ag nanoparticles by picosecond lift to improve the photoelectric property of AZO films," Chin. Opt. Lett. **18**, 043101 (2020).
18. J. Li, W. Yu, D. Zheng, X. Zhao, C.-H. Choi, and G. Sun, "Hot embossing for whole Teflon superhydrophobic surfaces," Coatings **8**, 227 (2018).
19. B. Parekh, S. Zheng, A. Entenberg, T. Debies, and G. A. Takacs, "Surface modification of poly(tetrafluoroethylene-co-hexafluoropropylene) with vacuum UV radiation from rotating helium dc arc plasmas," J. Adhes. Sci. Technol. **21**, 983 (2007).
20. N. I. Min'ko and V. M. Nartsev, "Factors affecting the strength of the glass," Middle East J. Sci. Res. **18**, 1616 (2013).
21. P. Kongsuwan, G. Satoh, and Y. Yao, "Transmission welding of glass by femtosecond laser: mechanism and fracture strength," J. Manuf. Sci. Eng. **134**, 011004 (2012).
22. D. Shen, J. Qian, C. Wang, G. Wang, X. Wang, and Q. Zhao, "Facile preparation of silver nanoparticles in bulk silicate glass by high-repetition-rate picosecond laser pulses," Chin. Opt. Lett. **19**, 011901 (2021).
23. N. Gupta, M. V. Kavya, Y. R. G. Singh, J. Jyothi, and H. C. Barshilia, "Superhydrophobicity on transparent fluorinated ethylene propylene films with nano-protrusion morphology by Ar + $O_2$ plasma etching: study of the degradation in hydrophobicity after exposure to the environment," J. Appl. Phys. **114**, 164307 (2013).
24. D. Clark, W. Feast, D. Kilcast, and W. Musgrave, "Applications of ESCA to polymer chemistry. III. Structures and bonding in homopolymers of ethylene and the fluoroethylenes and determination of the compositions of fluoro copolymers," J. Polym. Sci. Pol. Chem. **11**, 389 (1973).
25. M. Ackeret, "Polytetrafluoroethylene by XPS," Surf. Sci. Spectra **1**, 100 (1992).
26. S. Agraharam, D. W. Hess, P. A. Kohl, and S. A. Bidstrup Allen, "Plasma chemistry in fluorocarbon film deposition from pentafluoroethane/argon mixtures," J. Vac. Sci Technol. A. **17**, 3265 (1999).
27. G. L. Georgiev, R. J. Baird, E. F. McCullen, G. Newaz, G. Auner, R. Patwa, and H. Herfurth, "Chemical bond formation during laser bonding of Teflon® FEP and titanium," Appl. Surf. Sci. **255**, 7078 (2009).
28. D. Xia, L. M. Johnson, and G. P. López, "Anisotropic wetting surfaces with one-dimesional and directional structures: fabrication approaches, wetting properties and potential applications," Adv. Mater. **24**, 10 (2012).
29. Z. Cheng, D. Zhang, T. Lv, H. Lai, E. Zhang, H. Kang, Y. Wang, P. Liu, Y. Liu, Y. Du, S. Dou, and L. Jiang, "Superhydrophobic shape memory polymer arrays with switchable isotropic/anisotropic wetting," Adv. Funct. Mater. **28**, 1705002 (2018).
30. N. Gui, W. Xu, J. Tian, G. Rosengarten, M. Brandt, and M. Qian, "Fabrication and anisotropic wettability of titanium-coated microgrooves," J. Appl. Phys. **123**, 095306 (2018).